

745. D. Hutsemékers and E. Van Drom: HR Car: a Luminous Blue Variable Surrounded by an Arc-Shaped Nebula. *Astronomy and Astrophysics*.
746. G. Bertin, R.P. Saglia and M. Stiavelli: Elliptical Galaxies with Dark Matter. I. Self-Consistent Models. *Astrophysical Journal*.
747. H.M. Adorf, J.R. Walsh and R.N. Hook: Restoration Experiments at the St-ECF. Proc. Workshop "The Restoration of HST Images and Spectra", STScl, Baltimore, 21–22 August 1990.
748. L.B. Lucy: Restoration with Increased Sampling – Images and Spectra. Proc. Workshop "The Restoration of HST Images and Spectra", STScl, Baltimore, 21–22 August 1990.
748. P. Bouchet, J. Manfroid and F.-X. Schmider: JHKLM Standard Stars in the ESO System. *Astronomy and Astrophysics*.
749. P. Bouchet, I.J. Danziger and L.B. Lucy: The Bolometric Light Curve of SN 1987A: Results from Day 616 to 1316 After Outburst. *Astronomical Journal*.
750. G.A. Tammann: Commission 28: Galaxies. IAU Transactions, Vol. XXI A, 1991.
751. B. Reipurth and M. Olberg: Herbig-Haro Jets and Molecular Outflows in L 1617. *Astronomy and Astrophysics*.
752. B. Reipurth and S. Heathcote: The Jet and Energy Source of HH 46/47. *Astronomy and Astrophysics*.

Supermassive Disk Galaxies

L.M. BUSON, *Osservatorio Astronomico, Padova, Italy*

G. GALLETTA, *Dipartimento di Astronomia, Padova, Italy*

R.P. SAGLIA, *Department of Astrophysics, Oxford, United Kingdom*

W.W. ZEILINGER, *ESO*

Introduction

Supermassive disk galaxies (SDGs hereinafter) are characterized by a high rotational velocity of their gas component ($V_{\max} > 350 \text{ km s}^{-1}$). NGC 1961 (Shostak et al., 1982), UGC 2885 (Burstein et al., 1982) and UGC 12591 (Giovanelli et al., 1986) are the best known examples. As Saglia and Sancisi (1988) pointed out, these galaxies lie at the extreme upper end of the Tully-Fisher relation and are on the average less luminous than expected from their rotational velocity. Their mean mass-to-luminosity ratio M/L is 15 (with $H_0 = 75 \text{ Mpc km s}^{-1}$), i.e. 1.6 times the value for Sa galaxies (Rubin et al., 1985). In addition, their optical sizes appear to be on the average smaller than those of the normal galaxies.

SDGs have been discovered only recently, since in the past the technical limitations of the 21-cm spectrometers have rendered impossible the detection of the very wide HI profiles that characterize such systems. In effect, none of the galaxies in the Roberts (1978) sample has a rotational velocity greater than 350 km s^{-1} . SDGs are still poorly known: it is not even clear whether supermassive galaxies really form a distinct category of galaxies with definite properties or whether they simply represent the extreme tail of the distribution towards the largest masses. These questions have deep implications on the formation and evolution of galaxies and the amount of dark matter. The observed properties indicate that in supermassive galaxies dark matter may dominate even inside the R_{25} radius, in contrast to what seems to happen in normal spirals (Sancisi and van Albada, 1985).

Observations and Data Reduction

In order to investigate further these properties we have started an extensive optical survey of SDG candidates in the southern hemisphere, using the 2.2-m ESO/MPI telescope at La Silla. In particular, we would like to understand

whether SDGs have in general an unusual high content of dark matter in the inner regions or, perhaps, an unusual stellar population. It is important to study SDGs optically, since the distribution of HI often has a hole in the centre and is also affected by a severe beam

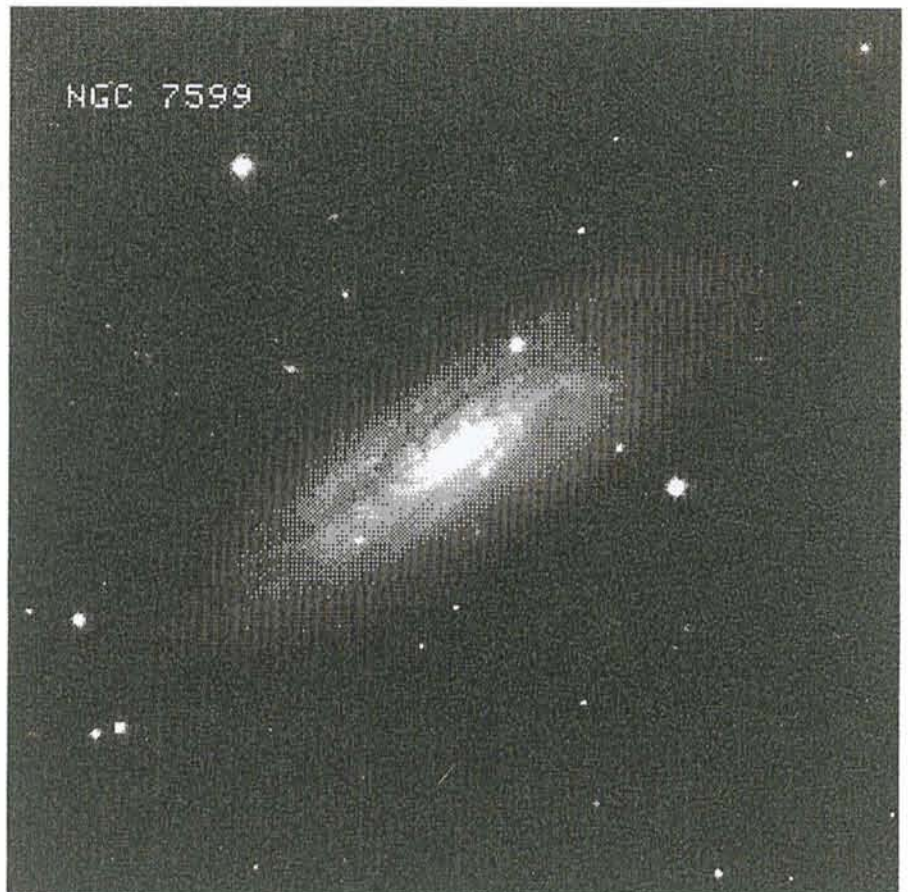


Figure 1: Red image of NGC 7599 obtained with EMMI at the NTT (kindly taken for us by S.D'Oodorico). The field is 6×6 arcmin. North is at the top and East to the right.

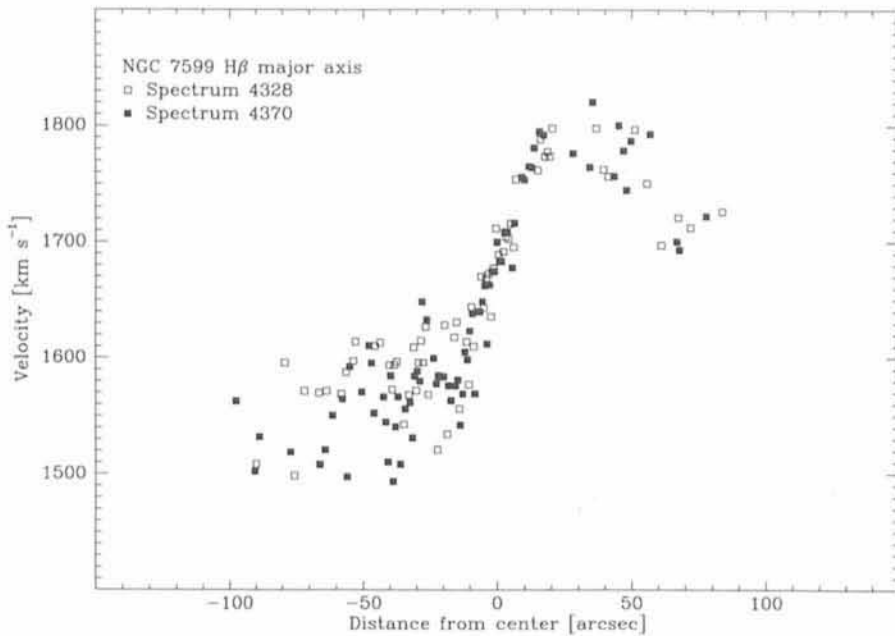


Figure 2: Rotation curve of the gaseous component of NGC 7599 derived from the measurements of the H β line at P.A. = 57°. The exposure time of each spectrum was 120 minutes.

smearing. Moreover, for the case of southern galaxies, high resolution HI observations are still lacking. A candidate list was produced using the HI catalogue of Huchtmeier and Richter (1989) and the following selection criteria: (i) a rotational velocity $V_{\text{max}} \geq 350 \text{ km s}^{-1}$, deduced from the HI line width at 20% height. (ii) a HI line profile quite regular and double-horned, indicating circular motions.

Our observations of SDGs started with NGC 5084, which was observed in May 1987 and July 1988 as a feasibility test of this programme. The results (Zeilinger, Galletta and Madsen, 1990) were so encouraging that we decided to start this work more systematically. CCD images in different colours, deep Schmidt plates and long-slit spectroscopy of four additional galaxies (NGC 1350, NGC 1398, NGC 7038, and NGC 7599) were then obtained in October 1990. A CCD image of NGC 7599 is presented in Figure 1 as an example. Other galaxies will be observed next April using again the 2.2-m telescope. The data reduction has been performed using IHAP and other specific programmes developed in Padova (Fourier-Quotient package). A sample rotation curve of the ionized gas, obtained by means of Gaussian fitting of the emission lines is shown in Figure 2 for the galaxy NGC 7599. Surprisingly the gas rotation curve of NGC 7599 has values which are too low for SDG. This may have two reasons: (i) we are looking only at the inner region of the galaxy and the rotation curve rises outside; (ii) the very wide HI profile is influenced by the presence of a companion galaxy or has too low an

S/N ratio. The analysis of the stellar rotation curve and the stellar velocity dispersion profile may clarify this point.

In order to analyse the luminosity distribution outside the region covered by the CCD frames we used ESO Schmidt plates and the calibrated images, extracted from the ESO-LV catalogue on optical disk (Lauberts and Valentijn, 1989). The inner parts of the galaxies have been calibrated in surface brightness using the aperture photometry values reported in the catalogue of Longo and de Vaucouleurs (1983).

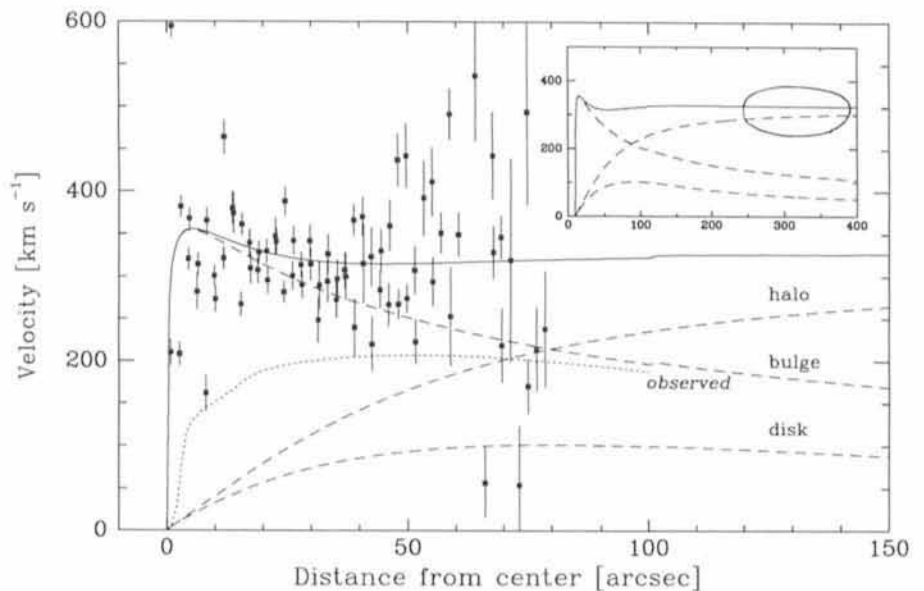


Figure 3: Rotation curve on NGC 5084 presented as the sum of bulge, disk and halo (dashed lines) in order to fit both the circular rotation curve (full line) and the velocities of the outer HI ring (shown in the inset as ellipse). The dotted line represents the observed rotation curve. The individual observed values (full points) are corrected for the asymmetric drift and integration along the line-of-sight.

The M/L Ratio: Models and Results

The relevant kinematical information comes from stellar and ionized gas rotation curves. Rotational velocities must be corrected for the inclination; the stellar rotation curves (obtained from absorption lines) also require a correction for the asymmetric drift, if a non-negligible velocity dispersion is present. In addition, the effect of integration along the line of sight must be taken into account (in the hypothesis of negligible absorption). More accurate corrections, taking into account the presence of internal absorption (Holmberg, 1958, Disney, 1990, Valentijn, 1990) will be included in the final paper. These corrections are accomplished with a three-component model (Zeilinger, Galletta and Madsen, 1990) representing the bulge, disk and halo component. A Young density law (Young, 1976) is used to reproduce the bulge halo $R^{1/4}$ component, an exponential law to simulate the disk, and a power law of the type discussed by van Albada et al. (1985) for the dark halo. This model yields a circular velocity curve (related to the mass density profile assuming that the luminous components of the galaxies have constant M/L ratios) and a light density profile. For NGC 5084 the corrected stellar rotation curve is in agreement with the velocities measured at 21-cm wavelength by Gottesman and Hawarden (1986) at a distance (400") twice the optical size of the disk. The global M/L profile of the galaxies can be derived from the above density profiles.

Figure 3 shows for NGC 5084 the decomposition of the observed rotation

curve into the contributions of bulge, disk and halo component. Combining these results with existing HI data, the extension of the halo component and its contribution to the total galaxy mass can be calculated. For instance, in the case of NGC5084, a massive halo is required to explain the M/L profile. This is found to vary from about $19 M_{\odot}/L_{\odot}$ ($H_0=100 \text{ Mpc km s}^{-1}$) in the inner regions increasing outwards to $45 M_{\odot}/L_{\odot}$, with a possible central peak of $> 30 M_{\odot}/L_{\odot}$. Following the model, a total mass of $7.28 \times 10^{11} M_{\odot}$ ($R < 30 \text{ kpc}$), 80% of which contained in the halo component, is derived. The presence of the massive halo could also explain the tilted lane observed in this galaxy in terms of a stabilized warped disk (Binney, 1978).

NGC5084 is an S0 galaxy, but nevertheless has an enormous quantity of gas. This observed gas can hardly derive from a single accretion event, since such a large mass would probably leave the gas in an inclined configuration due to the effect of self-gravitation

(Sparke and Casertano, 1988), but this configuration is not observed. If the picture of the external origin of the gaseous material should still hold, one has to assume that the time scale of the accretion process is very short with respect to the life time of the galaxy.

A possible picture for the formation of SDGs is then that they are the result of a series of accretion events, possibly induced also by the progressive deepening of the galaxy potential well.

References

Binney, J., 1978. *Mon. Not. R. Astr. Soc.*, **183**, 779.
 Burstein, D., Rubin, V.C., Thonnard, N. and Ford, W.K.Jr., 1982. *Astroph. J.*, **253**, 70.
 Disney, M., 1990. *Nature*, **346**, 105.
 Giovanelli, R., Haynes, M.P. and Chincarini, G.L., 1986. *Astroph. J.* **301**, L7
 Gottesman, S.T. and Hawarden, T.G., 1986. *Mon. Not. R. Astr. Soc.*, **219**, 759.
 Holmberg, E., 1958. *Medd. Lund Astr. Obs. Ser.*, 2, n. 136.

Huchtmeier, W.K. and Richter, O., 1989. *A General Catalog of HI Observations of Galaxies* (New York, Springer).
 Lauberts, A. and Valentijn, E.A., 1989. *The Surface Photometry Catalogue of the ESO-Uppsala Galaxies* (ESO, Garching).
 Longo, G. and de Vaucouleurs, A., 1983. *A General Catalog of Photoelectric Magnitudes and Colors in the U,B,V Systems*, Univ. Texas Monogr. Astron. n. 3.
 Roberts, M.S., 1978. *Astron. J.*, **83**, 1026.
 Rubin, V.C., Burstein, D., Ford, W.K.Jr. and Thonnard, N., 1985. *Astroph. J.*, **289**, 81.
 Saglia, R.P. and Sancisi, R., 1988. *Astron. Astrophys.*, **203**, 28.
 Sancisi, R. and van Albada, T.S., 1985. *IAU Symp.* **117**, 67.
 Shostak, G.S., Hummel, E., Shaver, P.A., van der Hulst, J.M. and van der Kruit, P.C., 1982. *Astron. Astrophys.*, **115**, 293.
 Sparke, L.S. and Casertano, S., 1988. *Mon. Not. R. Astr. Soc.*, **234**, 873.
 Valentijn, E.A., 1990. *Nature*, **346**, 153.
 van Albada, T.S., Bahcall, J.N., Begemann, K. and Sancisi, R., 1985. *Astroph. J.*, **295**, 305.
 Young, P.J., 1976. *Astron. J.*, **81**, 807.
 Zeilinger, W.W., Galletta, G. and Madsen, C., 1990. *Mon. Not. R. Astr. Soc.*, **246**, 324.

On the Origin of the Continuum Radiation at Optical and Ultraviolet Wavelengths in AGN/Quasars

M.-H. ULRICH, ESO

It is generally proposed that the energy source in quasars and Seyfert galaxies is accretion onto a massive object. Since angular momentum appears in most astrophysical situations, it has been further proposed that the accreted gas is assembled in a disk (Lynden-Bell, 1969; Shields, 1978; for reviews see Pringle, 1981; Collin-Souffrin and Lasota, 1988). For a given model, the spectrum of the radiation emitted by a pure viscous flow can be calculated. Comparison of this continuum spectrum with the observed optical/UV/soft X-ray spectrum can, in principle, give the mass of the central object M_{BH} and the accretion rate \dot{M} (e.g. Sun and Malkan, 1989). However, not only are the models still uncertain but also, as we shall see below, the rapid variations of the UV and optical continuum of AGN suggest that the origin of this continuum is more complex than previously realized.

Let us examine the flux variations data available for one of the best studied AGNs: NGC 4151 (Ulrich et al., 1990).

NGC 4151 has been observed with IUE on 125 days mostly grouped in campaigns of typically 20 to 40 days,

the interval between observations being 4 to 5 days. No ground-based optical observations were systematically done simultaneously with the UV observations but we have at our disposal the flux measured with the fine error sensor (FES) on-board IUE before each spectral exposure. The optical FES flux, which is recorded with an S20 photocathode, is contributed by variable components

(broad emission lines + continuum) and a nonvariable component including stellar light and narrow emission lines.

The contribution of the Balmer continuum in the FES band is negligible. That of the broad emission lines is estimated to be $< 20\%$ of the total flux.

Figures 1 and 2 show that the optical (FES) and UV fluxes undergo variations which are simultaneous within our time

TABLE 1: NGC4151 = Selected episodes: observing dates

1983	IUE EXOSAT	October 30; November 4, 7, 11, 15, 19 November 7, 11, 15, 19
1984	IUE EXOSAT	December 16, 19, 24, 28 December 16, 20, 22, 24, 28
1985	IUE EXOSAT	January 2, 8, 14 January 2
1988	IUE	November 29 December 10, 14, 20, 24, 28, 31
1989	IUE	January 5, 9, 13, 17, 21, 25, 30
1990	IUE	February 25 March 1, 5, 9, 13, 17, 21 April 1, 12, 17